EXPERIMENTAL CALIBRATION OF THE CONSTRAINING LINKAGE OF A 4 DEGREES OF FREEDOM PARALLEL MANIPULATOR

Leila Notash, Andrew Horne and Victoria Lee

Department of Mechanical and Materials Engineering, Queen's University, Kingston, ON, Canada
notash@me.queensu.ca horne@me.queensu.ca

Received June 2007, Accepted November 2007
No. 07-CSME-60, E.I.C. Accession 3029

ABSTRACT

In this article, an experimental calibration of the constraining linkage of a wire-actuated parallel robot is discussed. The experimental test bed includes a prototyped 4 degrees of freedom wire-actuated parallel manipulator and an optical tracking system. The parallel manipulator employs hybrid actuation of joints and wires and includes a rigid branch to constrain the motion of its mobile platform in roll and yaw rotations. The kinematic calibration of the rigid branch is performed. A point-to-point path is designed for the manipulator and an optical tracking system is used as an external measuring device to track a tool attached to the mobile platform and to register the manipulator poses. The deviation between the actual (measured) pose of the mobile platform and the calculated pose (via direct kinematics using the joint encoders), which could be due to errors in the kinematic parameters, actuators and sensors, is used as the error function.

Keywords: Parallel manipulator, kinematic calibration

ÉTALONNAGE EXPÉRIMENTAL D'UNE LIAISON CONTRAIGNANTE D'UN MANIPULATEUR PARALLÈLE DE MOBILITÉ À QUATRE DEGRÉS

RÉSUMÉ

Cet article traite d'un étalonnage expérimental d'une liaison contraignante d'un robot parallèle activé par un fil. Le banc d'essai expérimental comprend un manipulateur parallèle activé par un fil de liberté de quatre degrés prototypé et un système de suivi optique. Le manipulateur parallèle emploie une activation hybride de joints et de fils, et inclut une branche rigide pour contraindre le mouvement de sa plate-forme mobile en rotations de roulis et de lacet. L'étalonnage cinématique de la branche rigide est réalisé. Une trajectoire point à point est conçue pour le manipulateur et un système de suivi optique est utilisé comme appareil de mesure externe pour suivre un outil attaché à la plate-forme mobile et pour enregistrer les poses du manipulateur. L'écart entre la pose réelle (mesurée) de la plate-forme mobile et la pose calculée (par l'entremise de la cinématique au moyen d'encodeurs de joints), qui pourrait être attribuable aux erreurs des paramètres cinématiques, d'activateurs et de senseurs, est utilisé comme fonction d'erreur.

Mots-clés : Manipulateur parallèle, étalonnement cinématique

1. INTRODUCTION

Parallel robot manipulators consist of one or more closed-loops of links and joints where the mobile platform (end effector) is connected to the base by at least two kinematic chains (legs/branches). Because of the closed-loop configuration, in parallel manipulators not all of the joints are actuated and sensed. That is, in closed-loop manipulators the majority of the joints are passive and generally unsensed. This is because for an n degrees of freedom (DOF) parallel manipulator, a minimum of n independent joints have to be actuated (and sensed). This could result in challenges during the kinematic analysis and also calibration of parallel manipulators, because the terms relating to the motion of passive (and unsensed) joints need to be eliminated from the equations using the constraints due to the closed loops.

The goal of robot kinematic calibration is to obtain an accurate kinematic model of the manipulator in terms of link and joint parameters. Calibration of parallel manipulators is performed to reduce the error in the calculated mobile platform position and orientation (pose) by identifying errors of the kinematic and joint transducer parameters. Hence, precise measurement of the mobile platform pose is required, e.g., using an external measuring device, in order to quantify the pose error.

There are three main levels of robot calibration [1] which are: joint level calibration (to identify a correct relationship between the joint transducer signal and the joint displacement), geometric calibration (to identify the kinematic relation between the joints and links based on geometric parameters of the manipulator), and non-geometric calibration (to investigate gear backlash, link/joint compliance, friction and dynamic calibration).

Robot kinematic calibration procedure consists of four steps [2]. The first step is to construct a model of the robot manipulator, i.e., to determine the relationship between the joint displacements and the end effector pose. This is usually called the forward model, where the end effector pose is expressed using the joint displacements. The second step is precise measurement of the robot end effector pose using measuring devices such as coordinate measuring machines, laser interferometry, calibration fixture or camera. The third step is the identification of the discrepancies in the parameters of kinematic model from end effector measurements and joint displacement readings at these measured poses. The last step is to compensate for the errors in the robot controller, e.g., by modifying the control software.

Linear and nonlinear least squares techniques have been used in robot calibration to obtain estimates of the parameters to be identified. The error model based on the nonlinear manipulator kinematic model is generally differentiable. Therefore, gradient search algorithms can be applied, including steepest descent method (Newton-Raphson's algorithm), iterative non-linear least squares algorithm (Gauss-Newton algorithm), damped Gauss-Newton method (Levenberg-Marquardt algorithm), and so on.

The Denavit and Hartenberg (DH) parameters are commonly used for geometric modelling in robotics [3]. The DH convention uses a set of 4 parameters which describe the transformation from the reference frame of one link to the next. This creates a systematic method to model the mechanism from one link to the next. The DH convention uses a rotation about the z-axis (θ), translation along the z-axis (d), translation along the x-axis (a) and rotation about the x-axis (α). This method fails for robot calibration when two joint axes are nearly parallel. In this case a set of modified DH parameters can be used to achieve calibration [4]. The parameters used by the modified DH convention are slightly different then the DH convention; the parameter d is not used and a rotation about the y-axis (β) is included.

Several different treatments have been used for the calibration of closed-loop mechanisms. The use of loop closure equations as a constraint on the objective function was proposed in [5]. For the calibration of a planar 4-bar mechanism, in [6] it was discussed that the planar loop closure constraint function would result in a singular Jacobian and cannot be solved numerically. To avoid this difficulty, it was proposed that such a mechanism should be modelled as an ideally planar mechanism. It should be noted that if the joint axes of the mechanism are not perfectly aligned, then in order for the mechanism to function there will be stresses and deformations allowing for the motion.

In this article calibration of the constraining linkage of a wire-actuated parallel manipulator is performed. An optical tracking system (camera) is used to track a tool that is attached to the mobile platform of the manipulator. The tracking system identifies the pose of the manipulator with respect to the reference frame of the tracking system. The tracking system is mounted on a passive tripod, and hence, its position and orientation could be varied. The base of the manipulator is not within the workspace of the tracking system. Therefore, to identify the pose of the mobile platform with respect to the manipulator base frame, using the tracking system, another tool is defined within the workspace of the tracking system (on a nearby parallel robot, with a known pose). The transformations between the reference frame of the tracking system and the frames of the two tools are identified and utilized to calculate the pose of the manipulator with respect to its base frame. Then the collected data are used for the calibration of the constraining linkage of the manipulator using Levenberg-Marquardt method. The results verify the success of calibration.

2. SYSTEM DESCRIPTION AND MANIPULATOR MODEL

The considered wire-actuated parallel manipulator (Figure 1) has 4 DOF, and includes a rigid branch (with seven joints) and three wires [7]. The rigid branch is employed to constrain the undesired motions of the mobile platform, i.e., the roll and yaw rotations, and it connects the center of the mobile platform to the base. The rigid branch consists of a parallelogram mechanism (a 1 DOF mechanism) which is connected to the base via an actuated revolute joint (1 DOF). The coupler link of the parallelogram mechanism is connected to the mobile platform via an intermediate link and two revolute joints (2 DOF). Two joints of the rigid branch, i.e., the joints closest to the base (joints j_1 and j_2), are actuated. The two revolute joints that connect the parallelogram mechanism to the mobile platform (joints j_4 and j_5) are only equipped with encoders, i.e., these joints are not actuated. The motions of these two revolute joints are controlled by three wires as wires could only pull (not push). The pose of the mobile platform could be identified using the encoders on the independent joints (joints j_1, j_2, j_4 and j_5) of the rigid branch.

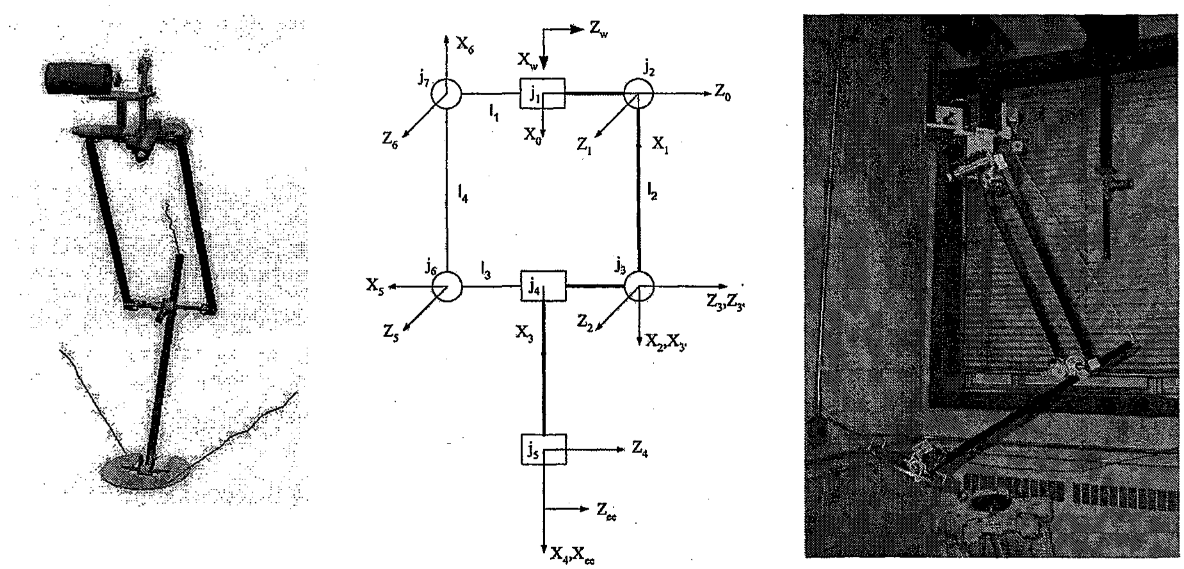

(a) (b) (c)

Figure 1: Wire-actuated manipulator: (a) solid model [7], (b) simplified diagram [8], (c) prototyped.

Table 1 Denavit-Hartenberg parameters of the constraining linkage.

From Frame	θ_i	d_i	a_i	α_i	β_i	To Frame
0	θ_1	d_1	a_1	α_1	0	1
1	θ_2	0	$a_2 = l_2$	α_2	β_2	2
2	θ_3	d_3	a_3	α_3	0	3′
3′	0	$d_{3'}$	0	0	0	3
3	θ_4	0	a_4	α_4	β_4	4
4	θ_5	0	a_5	α_5	β_5	ee

The pose of reference frame for the first link ($X_0Y_0Z_0$) is expressed with respect to the global frame using six parameters. Denavit-Hartenberg parameters (θ_i, d_i, a_i, α_i) [3] are used for modelling the joints of the manipulator. For the calibration model of parallel joint axes, the modified DH method (θ_i, a_i, α_i, β_i) is used [9]. Table 1 includes the list of parameters for the constraining linkage. In order to include the distance between the origins of coordinate frames for joints j_3 and j_4 (labelled in Figure 1) in the DH table, the dummy frame $X_{3'}Y_{3'}Z_{3'}$ is utilized. Otherwise, this distance would be along the Y_2 axis. The parallelogram mechanism is modelled as a planar mechanism for deriving the relation for the dependent joint $\theta_3 = -\theta_2$, hence, the four revolute joint axes are parallel and the links are all perpendicular to the corresponding joint axes. As well, joints j_1 and j_4 are modelled to be collinear with the base and coupler links of the parallelogram mechanism respectively. That is, $\alpha_1 = 90°$, $\alpha_2 = 0$ and $\beta_2 = 0$ and $\alpha_3 = -90°$. The out of plane offset of the linkage is modelled by d_3. The dependency of a_1 and $a_{3'}$ is taken into account by means of $a_1 = 0$, as they are in the same direction. Parameter d_1 is kept constant while $d_{3'}$ is calibrated.

The transformation matrix between two adjacent reference frames is formed using the basic transformations as:

$$A_{i-1,i} = \boldsymbol{Rot}(z,\theta_i)\boldsymbol{Trans}(z,d_i)\boldsymbol{Trans}(x,a_i)\boldsymbol{Rot}(x,\alpha_i) \tag{1}$$

$$A_{i-1,i} = \boldsymbol{Rot}(z,\theta_i)\boldsymbol{Trans}(x,a_i)\boldsymbol{Rot}(x,\alpha_i)\boldsymbol{Rot}(y,\beta_i) \tag{2}$$

where equation (1) relates to the DH parameters and equation (2) corresponds to the modified DH parameters (parallel revolute joint axes of branch).

The actuators of the manipulator are controlled using a Q8 data acquisition board (from Quanser Consulting Inc.), which is installed on the motherboard of a Pentium III/1.0 GHz host computer, and WinCon™ real-time Windows 2000/XP based software. The encoders of the actuated joints (j_1 and j_2 in Figure 1) have a resolution of 500 pulses per revolution (ppr). The motors that are used to actuate these joints have an internal gear reduction ratio of 134:1, and an external gear transmission is used with a gear ratio of 4:1. Therefore, the resolution of these two encoders is 268,000 ppr. The resolution of the encoders of the passive joints four and five (j_4 and j_5 in Figure 1) are respectively 1000 and 200 cycles per revolution (with four pulses per one cycle). An external gear transmission is used for these two encoders, where the gear ratio for joint four is 1.6:1 and for joint five is 0.997:1. It should be noted that even though two identical gears were used in the gear train of joint five, 0.997:1 was obtained during joint level calibration when the joint was moved to known positions and the encoder reading was measured (wear and tear effect). The data acquisition system has quadrature mode, i.e., for joints four and five it could get 6400 and 797.600 counts per revolution after the quadrature decoding.

The Polaris tracking system (from Northern Digital Inc.) has a position sensor to measure the position of the infrared light that is reflected from the markers on the tool. The root-mean-square (RMS) volumetric acceptance criterion for the Polaris is reported to be 0.350 mm (based on a single marker stepped through over 1200 positions throughout the defined workspace, using the mean of 30 samples at each position, at 20°C) [10]. The resolutions of the encoders and the RMS error of the tracking system dictate the accuracy level of the calibration.

3. MANIPULATOR PARAMETER IDENTIFICATION

Due to the manufacturing (fabrication and assembly) tolerances and also non-geometric errors such as gear backlash, there is an inconsistency between the measured mobile platform pose $\boldsymbol{r}$ and the pose calculated from kinematic model $\boldsymbol{r}_c(\boldsymbol{q},\boldsymbol{a})$. The error vector of mobile platform pose in the *j*th measurement can be formulated as

$$\boldsymbol{e}_j = \boldsymbol{r}_j - \boldsymbol{r}_c(\boldsymbol{q}_j, \boldsymbol{a}) \tag{3}$$

where $\boldsymbol{r}_j$ is the mobile platform pose in the *j*th measurement, $\boldsymbol{q}_j$ is the vector of joint displacements, and $\boldsymbol{a}$ is the vector of kinematic parameters. The objective is to identify the discrepancies in the kinematic and joint parameters such that the following expression is minimized for all manipulator poses

$$\sum_{j=1}^{m} \boldsymbol{e}_j^T \boldsymbol{e}_j \tag{4}$$

where m is the total number of measured mobile platform poses. Expression (4) is a nonlinear function of kinematic and joint parameter errors. This expression could be linearized using the Taylor series expansion, or a nonlinear function minimization approach may be employed to identify the desired errors.

Assuming small errors, i.e., neglecting the second and higher order differential terms, the error vector reduces to

$$\boldsymbol{e}_j = \frac{\partial \boldsymbol{r}_c(\boldsymbol{q}_j,\boldsymbol{a})}{\partial \boldsymbol{q}} \delta \boldsymbol{q} + \frac{\partial \boldsymbol{r}_c(\boldsymbol{q}_j,\boldsymbol{a})}{\partial \boldsymbol{a}} \delta \boldsymbol{a} \tag{5}$$

Equation (5) is linear with respect to the joint errors $\delta\boldsymbol{q}$ and parameter errors $\delta\boldsymbol{a}$. The mobile platform pose error for all of the measured poses can be written as

$$\boldsymbol{e}_{ag} = \begin{bmatrix} \boldsymbol{J}_1 \\ \vdots \\ \boldsymbol{J}_m \end{bmatrix} \begin{bmatrix} \delta \boldsymbol{q} \\ \delta \boldsymbol{a} \end{bmatrix} = \boldsymbol{J}_{ag} \delta \boldsymbol{c}_{ag} \tag{6}$$

where $\boldsymbol{e}_{ag} = \begin{bmatrix} \boldsymbol{e}_1^T & \cdots & \boldsymbol{e}_m^T \end{bmatrix}^T$, $\boldsymbol{J}_{ag}$, $\delta\boldsymbol{c}_{ag}$ are respectively the $6m \times 1$ aggregated mobile platform pose error, the $6m \times p$ aggregated identification Jacobian matrix and the $p \times 1$ aggregated vector of parameter errors, and $\boldsymbol{J}_j$ is the identification Jacobian matrix at the *j*th measurement. The least-squares solution of equation (6) is the set of parameters that minimizes $(\boldsymbol{e}_{ag} - \boldsymbol{J}_{ag}\delta\boldsymbol{c}_{ag})^T(\boldsymbol{e}_{ag} - \boldsymbol{J}_{ag}\delta\boldsymbol{c}_{ag})$ and can be obtained as $\delta\boldsymbol{c}_{ag} = \boldsymbol{J}_{ag}^{+}\boldsymbol{e}_{ag}$ where $\boldsymbol{J}_{ag}^{+} = (\boldsymbol{J}_{ag}^T\boldsymbol{J}_{ag})^{-1}\boldsymbol{J}_{ag}^T$ is the generalized inverse of $\boldsymbol{J}_{ag}$. In the Levenberg-Marquardt method, which is based on the gradient vector and Hessian matrix of the objective function, at the *k*-th iteration, equation (6) is replaced by

$$\boldsymbol{J}_k^T (\boldsymbol{e}_{ag})_k = \left(\boldsymbol{J}_k^T \boldsymbol{J}_k + \mu_k \boldsymbol{I}\right) \boldsymbol{v}_k \tag{7}$$

where J_k is the $6m \times p$ aggregated identification Jacobian of the mobile platform pose error function, $\mu \geq 0$ is a scalar, I is a $p \times p$ identity matrix, and vector v_k indicates the direction of search [11].

4. EXPERIMENT DESIGN

The joint level calibration is performed by calculating the gains of the encoders based on the quadrature mode of data acquisition board, resolution of the encoders and gear reduction ratios as discussed in Section 2. That is, the displacements θ of joints one, two, four and five in terms of the corresponding encoder signal η are respectively

$$\theta_1 = \frac{2\pi}{4 \times 500 \times 134 \times 4}\eta_1 \tag{8}$$

$$\theta_2 = \frac{-2\pi}{4 \times 500 \times 134 \times 4}\eta_2 \tag{9}$$

$$\theta_4 = \frac{2\pi}{4 \times 1000 \times 1.690}\eta_4 \tag{10}$$

$$\theta_5 = \frac{-2\pi}{4 \times 200 \times 0.997}\eta_5 \tag{11}$$

For the kinematic calibration, the pose of the mobile platform could be fully described by the readings of the four encoders of the rigid branch, i.e., the two encoders of the actuated joints (j_1 and j_2) and the two encoders of the passive joints (j_4 and j_5). As well, the pose of the mobile platform could be measured by an external measuring device such as a Polaris optical tracking system by placing markers on the mobile platform. The emitted infrared light of the position sensor of the tracking system is reflected back by the markers to the optical receptors. Based on the reflected infrared light, the poses of markers, and hence the pose of mobile platform, are identified.

Designing the relative distances between the markers and the reference frame for the markers is called tool characterizing. The markers of the characterized tool should form a unique geometry so that the tracking system could identify the tool and find its pose. That is, a minimum of three markers are required, each pair of markers being apart by at least 50 mm while the distance between any two markers is different than the others by at least 5 mm [12].

For the wire-actuated parallel manipulator, three markers (*A*, *B* and *C*) are used on the mobile platform. The origin of mobile platform frame (tool) lies on the plane of mobile platform. It should be noted that the plane passing through the centers of the three markers, which is parallel to the plane of mobile platform, is shifted by 24.5 mm in $-Y_{ee}$ direction. As depicted in Figure 2(a), the origin of $X_{ee}Y_{ee}Z_{ee}$ frame is below marker *A* with Y_{ee} axis being normal to the plane of markers. The axes of the mobile platform frame are parallel to the fixed frame $X_0Y_0Z_0$ at the base of the manipulator when the constraining linkage is fully extended downward and the mobile platform plane is vertical. The pose of the mobile platform frame is identified by these three markers, positioned on the mobile platform based on the requirements of the NDI Architect software of Polaris for defining the tools to be tracked. The coordinates of these markers with respect to frame $X_{ee}Y_{ee}Z_{ee}$ are as follows: *A* (0, –24.500, 0), *B* (–34.231, –24.500, –84.272), and *C* (–118.570, –24.500, 118.569). The tracking system uses the three markers and reports the pose of frame $X_{ee}Y_{ee}Z_{ee}$.

In order to obtain the mobile platform pose with respect to the base coordinate frame, two tools are needed, one on the mobile platform of the wire-actuated manipulator and one to define the base (global) frame. The reference frame of the tracking system is not used for the measurements as Polaris is mounted on a passive tripod where its position and orientation could be varied (will not be the same for different measurements in case it is moved during experiment and data collection). Because the base of the wire-actuated manipulator is not accessible for putting markers and also it does not lie within the workspace of Polaris, a tool is defined on another parallel manipulator (FANUC F200*i*) which is located below the wire-actuated parallel manipulator. The mobile platform of F200*i* parallel robot at its home position (when the lengths of its prismatic joints are 668 mm) is within the workspace of Polaris. The tool of F200*i* is also characterized by three markers. As illustrated in Figure 2(b), the plane of markers is defined as XY plane, which is about 22.7 mm above the mobile platform plane of F200*i*. The origin of the reference frame is located at the center of marker *E* with markers *E* and *F* positioned on the X_{f200} axis. The coordinates of these markers with respect to the $X_{f200}Y_{f200}Z_{f200}$ frame are as follows: *D* (60.255, 104.691, 0), *E* (0, 0, 0), and *F* (87.893, 0, 0).

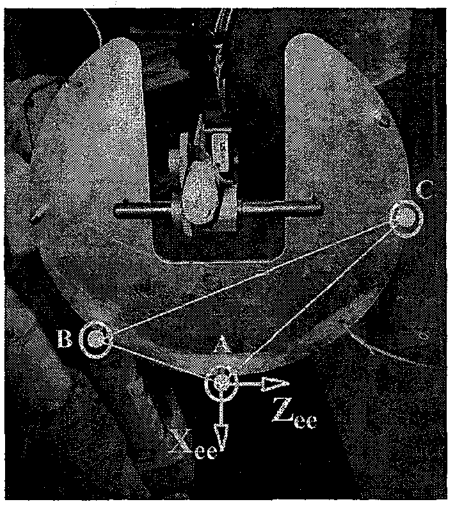

(a)

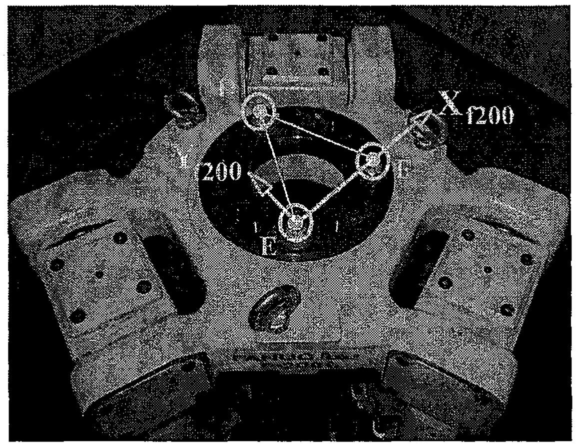

(b)

Figure 2: Three passive markers on mobile platform of (a) wire-actuated manipulator, (b) F200*i* robot.

5. IDENTIFICATION

As mentioned earlier, the deviation between the measured pose of the mobile platform of the wire-actuated parallel manipulator and the calculated pose (via direct kinematics using the joint encoders) is used as the error function. The manipulator poses are selected uniformly within its workspace. The optical tracking system is used to follow the mobile platform of the wire-actuated manipulator and display the pose (roll, pitch, yaw, p_x, p_y, p_z) with respect to the reference frame which was defined on the mobile platform of the F200*i* (global frame). The nominal transformation between the global reference frame and the base of the manipulator was determined experimentally, and the corresponding parameters were included in the calibration algorithm with the nominal values used as a starting point.

Using Polaris measurements of the two tools (one on the wire-actuated manipulator, one on the F200*i* robot) and the known pose of the wire-actuated manipulator at certain configurations based on the nominal values of its parameters, e.g., its zero-configuration when all joint displacements are zero), the measured poses of the wire-actuated manipulator with respect to the F200*i* tool are converted to the corresponding poses relative to the base coordinate frame of the manipulator. The nominal constant transformation from the base frame of wire-actuated parallel manipulator to the tool on F200*i* (at its home position), $A_{0,F200}$, is determined experimentally using

$$A_{0,ee} = A_{0,F200} A_{F200,ee} \quad (12)$$

Table 2 Seven poses of wire-actuated manipulator used for identifying nominal $A_{0,F200}$.

Pose #	Pitch (rad)	p_x (mm)	p_y (mm)	p_z (mm)
1	0	1209.250	0	0
2	−1.571	1090.650	−118.600	0
3	−0.524	1128.685	−300.675	0
4	−0.524	1193.361	−59.330	0
5	0	1127.807	303.950	0
6	−1.571	1009.207	185.350	0
7	0	1128.957	0	303.950

where the mobile platform pose of manipulator with respect to its base frame, $A_{0,ee}$, is calculated for the nominal DH parameters of the rigid branch for the known poses of manipulator. The relative position of the tool of wire-actuated manipulator with respect to the tool of F200*i*, $A_{F200,ee}$, is measured by Polaris. The measurements are carried out for seven different poses of manipulator (Table 2) and the calculated seven poses (roll, pitch and yaw angles and three translational coordinates) of the F200*i* tool with respect to the base frame are averaged to obtain the nominal constant transformation $A_{0,F200}$ as

$$A_{0,F200} = \begin{bmatrix} -0.0144 & 0.0136 & -0.9998 & 1095.231 \\ 0.5813 & -0.8135 & -0.0194 & 212.571 \\ -0.8136 & -0.5814 & 0.0038 & -293.864 \\ 0 & 0 & 0 & 1 \end{bmatrix} \quad (13)$$

The nominal $A_{0,F200}$ transformation results in a translation of 1095.231 mm, 212.571 mm and −293.864 mm in the X, Y, and Z directions, respectively. The rotation associated with the nominal $A_{0,F200}$ transformation is respectively −1.564 rad, 0.950 rad and 1.596 rad about X, Y, and Z directions. These parameters are denoted as X, Y, Z and Rx, Ry and Rz when reporting the calibration results. As well, a root-mean-square minimization is applied on the roll-pitch-yaw Euler angles and position coordinates and the resulting $\mathbf{A}_{0,F200}$ is very close to its expression in (13).

Two sets of data are collected during the measurement process; one using the data acquisition board (four encoder readings) and one based on the Polaris tracking system. Because of the time lag between the two measuring devices, and also since the data acquisition collects data for the whole duration of the data collection process while Polaris measurements are only for the discrete poses, some manipulation (filtering, analysis and reformatting) of data are required before they could be ready for the identification process. A Matlab program was written using the fmincon function to run the nonlinear constrained minimization. To ensure the correct minimum is found, the translational and rotational geometric parameters of the manipulator were constrained respectively to be within 10 mm and 0.100 radians. Because there is a lower level of confidence for the transformation from the global reference frame to the base of the manipulator, the corresponding constraints were relaxed to be 20 mm for translation and 0.200 radians for rotation.

The parameters that were kept constant during calibration (using a planar model for the parallelogram mechanism) are: d_1 = 104.85 mm, $a_1 = 0$, $\alpha_1 = 90°$, $\alpha_2 = 0$, $\beta_2 = 0$, $\alpha_3 = -90°$ and $\delta\theta_{3'} = 0$, where $\delta\theta_i$

represents the constant error (offset) in displacement of joint i (to account for error in the reference position for encoders). In addition, considering the position and orientation of frame $X_0Y_0Z_0$, six parameters were calibrated. This results in 20 independent parameters to be calibrated (14 parameters for the linkage and 6 parameters for the base frame). The results are reported in Table 3 (root-mean-square errors before and after calibration) and Table 4 (nominal and identified values of parameters) for 60 poses. As it can be seen from Table 3, the root-mean-square errors in translation and rotation have been reduced by 60.3% and 37.1% respectively. These results are very encouraging as during measurements some errors were introduced. For example, all the four encoders are relative (incremental) type and they need a reference position for their readings. At the start of tracking, the rigid branch of the manipulator was positioned as close to its zero-configuration (when all revolute joints have zero rotation) as possible and then the readings of the encoders were recorded relative to this configuration. Table 4 indicates that the nominal transformation from the global reference frame to the base of the manipulator was reasonably accurate because the calibrated parameters show changes within 20 mm for translation and 0.100 radians for rotation.

Table 3 Root-mean-square errors of mobile platform pose (60 poses).

	Initial	**Final**
RMS Error - Translation (mm)	14.204	5.635
RMS Error - Orientation (rad)	0.035	0.022

Table 4 Nominal and identified parameters of rigid branch for 60 poses.

Parameter	**Nominal**	**Updated**	**Change**	**Parameter**	**Nominal**	**Updated**	**Change**
X (mm)	1095.231	1081.263	13.268	a_3 *(mm)*	0	–9.647	9.647
Y (mm)	212.571	231.071	–18.500	$d_{3'}$ *(mm)*	–104.850	–103.621	–1.223
Z (mm)	–293.864	–294.556	0.692	$\delta\theta_4(rad)$	0	–0.086	0.086
Rx (rad)	–1.564	–1.534	–0.030	$a_4(mm)$	482.750	492.750	–10
Ry (rad)	0.950	0.938	0.012	$\alpha_4(rad)$	0	–0.005	0.005
Rz (rad)	1.596	1.621	–0.025	$\beta_4(rad)$	0	0.006	–0.006
$\delta\theta_1(rad)$	0	0.077	–0.077	$\delta\theta_5(rad)$	0	–0.030	0.030
$\delta\theta_2(rad)$	0	–0.019	0.019	$a_5(mm)$	118.600	119.421	–0.821
a_2 *(mm)*	607.900	597. 900	10	$\alpha_5(rad)$	0	–0.001	0.001
d_3 *(mm)*	0	10	–10	$\beta_5(rad)$	0	0.017	–0.017

6. VERIFICATION

In order to verify that the parameters identified during the calibration improve the accuracy of the manipulator, 49 additional pose measurements were used. The results of this verification can be seen in

Table 5. The error of these 49 poses using the nominal parameters is similar to the initial error of the 60 identification poses (Table 3) with the same nominal parameters. The parameters identified using the 60 poses (Table 4) were then applied to the 49 verification poses. This showed a significant improvement in the accuracy; the root-mean-square of the error improved by 37.4% for translation and 36.4% for rotation. As it would be expected, this is slightly lower than the improvement in the 60 poses used for the calibration.

Table 5 Root-mean-square errors of mobile platform pose, 49 verification poses.

	Nominal Parameters	**Calibrated Parameters**
RMS Error - Translation (mm)	16.217	10.155
RMS Error - Orientation (rad)	0.033	0.021

7. CONCLUDING REMARKS

This article concentrated on the experimental calibration of the constraining linkage (rigid branch) of a wire-actuated parallel manipulator. The manipulator utilizes redundancy in sensing (in addition to redundancy in actuation); hence all the independent joints of the rigid branch are sensed. This enables calibration of the rigid branch independent from the wire mechanism, as the pose of the mobile platform could be calculated utilizing the encoder readings of the two actuated and the two sensed passive joints of the branch. The results are very encouraging taking into account the RMS accuracy of Polaris and the measurement errors for the reference position of relative encoders. The calibrated parameters were verified against a separate set of poses demonstrating that the geometric calibration has been successful.

REFERENCES

1. Roth, Z.S., Mooring, B.W., and Ravani, B., Overview of Robot Calibration. *IEEE Trans. Robotics and Automation*, 3(5):377-385, 1987.
2. Mooring, B.W., Roth, Z.S., and Driels, M.R., *Fundamentals of Manipulator Calibration*, John Wiley, 1991.
3. Paul, R.P., Robot Manipulators: Mathematics, Programming, and Control; the Computer Control of Robot Manipulators, MIT Press, 1981.
4. Hayati, S.A., Robot Arm Geometric Link Parameter Estimation, Proc. 22nd *IEEE Conf. Decision and Control,* pages 1477-1483, 1983.
5. Everett, L.J., Lin, C.Y., Kinematic Calibration of Manipulators with Closed Loop Actuated Joints, Proc. *IEEE Conf. Robotics and Automation*, pages 792-797, 1988.
6. Schroer, K., Albright, S.L., Lisounkin, A., Modeling Closed-loop Mechanisms in Robots for Purposes of Calibration, *IEEE Trans. Robotics and Automation,* 13(2):218-229, 1997.
7. Mroz, G., and Notash, L., Design and Prototype of Parallel, Wire-Actuated Robots with a Constraining Linkage, *J. Robotic Systems*, 21(12):677-687, 2004.
8. Varziri, M.S., and Notash, L., Kinematic Calibration of a Wire-Actuated Parallel Robot, *Mechanism and Machine Theory,* 42(8):960-976, 2007.
9. Notash, L., Podhorodeski, R.P., Fixturless Calibration of Parallel Manipulators, *Trans. of CSME*, 21(3):273-294, 1997.
10. Polaris System User's Guide, Version 1.0, Northern Digital Inc., 2002.
11. Press, W.H., Teukolsky, S.A., Vetterling, W.T., and Flannery, B.P., *Numerical Recipes in C.* Cambridge University Press, 1992.
12. NDI 6D Architect User's Guide, Version 1.0, Northern Digital Inc., 2003.